ACS OMEGA

Open Access

http://pubs.acs.org/journal/acsodf

Article

Study on Pyrolysis and Oxidation Characteristics of Coal Gangue Based on TGA-DSC

Yongfei Jin, Dailin Li,* Yin Liu, Jun Guo, Changming Chen, and Xubin Yan

Cite This: *ACS Omega* 2024, 9, 14174−14186

Read Online

ACCESS | Metrics & More | Article Recommendations

ABSTRACT: Coal gangue spontaneous combustion has caused serious environmental and ecological problems. To investigate the reaction kinetic parameters of the gangue and the exothermic characteristics of the spontaneous combustion of the influence of the law, this study employs the thermogravimetric method to explore the characteristic parameters of the pyrolysis and oxidative combustion process of the gangue from the perspective of thermodynamics, and, at the same time, using the differential scanning calorimetry (DSC) on the exothermic effect of the gangue to explore the gangue to obtain the gangue and the original coal TG/DTG/DSC curves to be compared and from the perspective of thermodynamics. The change rule and potential parameters in the pyrolysis and oxidative combustion process of coal gangue (CG) were analyzed, the oxidation kinetic properties of CG were studied, and the reaction mechanism of oxidative spontaneous combustion of CG was further explained. The results show that the TG/DTG/DSC curves of CG in different gas atmospheres will have significant differences in all stages, and in the process of pyrolysis and oxidative combustion, the thermogravimetric curves of CG and those of the original coal show a consistent trend, except for the large difference in peak amplitude in different stages; in different gas atmospheres, as the rate of warming increases, the TG/DTG/DSC curves of the gangue are tilted toward the high-temperature region, they are inclined to the high-temperature region with the increase of the heating rate, and the phenomenon of "hysteresis" of characteristic temperature occurs. The research results provide a theoretical basis for the construction of a spontaneous combustion early warning system based on the fine division of gangue pyrolysis and oxidation combustion stages.

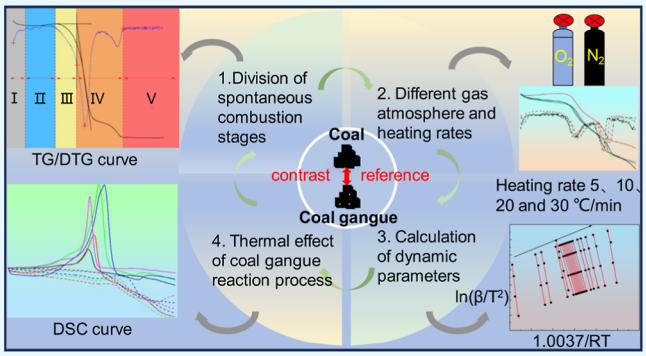

1. INTRODUCTION

Coal gangue (CG) is currently one of the largest source of annual emissions and accumulation of industrial waste in China; in the coal production process, gangue emissions account for about 15−25% of coal production, and the annual emissions are about 450 million tons.[1−3] There are over 1500 CG piles piled up in state-owned key coal mines, of which 389 have long-term spontaneous combustion. The natural ignition of CG will not only lead to the generation of large amounts of toxic and harmful gases but also easily cause gangue mountain collapses, blowouts, and explosions.[4−6] Therefore, it is necessary to analyze the nature and thermal effect of gangue pyrolysis and oxidative combustion process in the whole and at all stages, so as to reveal the spontaneous combustion mechanism of the gangue reaction process and to lay the foundation for the adoption of effective spontaneous combustion control measures for gangue.

CG is a complex mixture, which has the characteristics of low carbon and high ash content, low calorific value, and difficult combustion, which is different from coal's oxidation pyrolysis and combustion characteristics.[7−10] Recently, many scholars have studied the oxidation pyrolysis process and thermodynamics of CG spontaneous combustion and achieved fruitful results.[11,12] For example, Ran et al.[13] used thermal analysis technology to study CG from four different production areas and obtained the characteristic parameters of the pyrolysis reaction process of CG, such as activation energy, mechanism function, etc. The experimental results showed that reaction temperature, CG particle size, CG production area, and heating rate all had an influence on the pyrolysis reaction process of CG. Pu et al.[14] tested the combustion performance of gangue and its mixtures using thermogravimetric analysis and found that there is a significant heat loss in gangue during combustion, and its ignition temperature is higher, resulting in poor overall combustion performance. Wang, Ma, and Zhang[15] used nonisothermal

Received: December 6, 2023
Revised: January 3, 2024
Accepted: February 29, 2024
Published: March 15, 2024

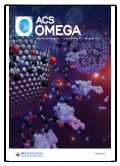

thermogravimetry to test the pyrolysis process of three different origins and particle sizes of CG under different atmospheric conditions. Jia and Yu[16] studied the effect of different oxygen concentration and heating rate conditions on the adiabatic oxidation process of CG by using a comprehensive thermal analyzer and derived the specific weight loss stages and weight loss characteristic points of the adiabatic oxidation process of CG. Wang et al.[17] used gas chromatography and mass spectrometry to carry out temperature-programmed experiments on CG samples of different pyrolysis grades. The results showed that there was a relationship between the pyrolysis grade of CG and its emission behavior and thermodynamic parameters, and the energy required for combustion of the sample after preheating was significantly higher than that of the original sample. In summary, different scholars have conducted in-depth studies on the oxidation and pyrolysis characteristics of CG under the influence of various factors such as different origin, particle size, heating rate, and gas atmosphere and explored the mechanism of natural ignition of CG.[18−22] However, the material composition of the CG is relatively complex, which is closely related to the physical and chemical characteristics of coal in its producing area. Therefore, it is necessary to compare and analyze the similarities and differences in the oxidative pyrolysis characteristics between CG and coal in the same producing area in order to reveal the spontaneous combustion law of CG and lay the foundation for the prevention and control of spontaneous combustion of the gangue mountain.

In this paper, thermogravimetric analysis/differential scanning calorimetry (TGA-DSC) was used to investigate the exothermic effect of CG, and the thermogravimetric curve and temperature evolution law of CG under different gas atmospheres and at different heating rates were discussed. In addition, the thermogravimetric curves of CG and raw coal were compared to reveal the pyrolysis and oxidation characteristics of CG, and the kinetic parameters of CG were solved using the Starink equation. It lays a good theoretical foundation for the prevention and control of coal gangue spontaneous combustion (CGSC), and it has important practical significance for the disaster prevention and control of CGSC and the protection of ecology and environment.

2. EXPERIMENTAL SECTION AND METHODS

2.1. Raw Materials. Raw coal and CG sampled from the Cuimu Coal Mine were sealed with woven bags and stored in the lab and laid flat to let them stand for a week at a normal temperature. After the surface dried up, the CG sample was broken up into 120−200 meshes with a crusher to make the test sample. For the proximate analysis of test samples, the moisture, ash, volatiles, and fixed carbon in the samples were tested using a 5E-MAG6700 Proximate analyzer; see Table 1 for the test results.

2.2. Test Conditions. The samples were tested for TGA-DSC using a Swiss METTLER TOLEDO STA (Simultaneous Thermal Analyzer) to get the TG/DTG/ DSC curve during the oxidation of the coal sample. The test philosophy was to continuously measure how the material mass is subjected to change with the temperature using a computer with a programmed thermostat controller.

To test the autoignition features of the samples, non-isothermal (dynamic) thermogravimetry was performed for thermal analysis of CG with a particle size of 120−200 mesh[23,24] at different heating rates in different gas atmospheres. The test conditions of the specific samples are listed in Table 2.

Table 1. Proximate Analysis Results

sample	proximate analysis/(%)			
	M_{ad}	A_{ad}	V_{ad}	FC_{ad}
CG	8.48	46.28	21.01	24.23
coal	10.35	6.87	26.33	56.45

Table 2. Test Conditions for Samples under Different Heating Rates

name		testing conditions	
		CG	Coal
air atmosphere	number of samples	5 ± 0.5 mg	5 ± 0.5 mg
	heating rate	5, 10, 20 and 30 °C/min	5 °C/min
	gas flow rate	50 mL/min	50 mL/min
	temperature range	30 °C ∼ 900 °C	30 °C ∼ 900 °C
nitrogen atmosphere	number of samples	5 ± 0.5 mg	5 ± 0.5 mg
	heating rate	5, 10, 20 and 30 °C/min	5 °C/min
	gas flow rate	50 mL/min	50 mL/min
	temperature range	30 °C ∼ 900 °C	30 °C ∼ 900 °C

3. RESULTS AND DISCUSSION

3.1. Thermogravimetric Curve and Characteristic Temperature of CG in Different Atmospheres. CG was tested at the heating rates of 5, 10, 20, and 30 °C/min in air and nitrogen atmospheres,[24,25] and the test results were compared with those of raw coal at a heating rate of 5 °C/min. The TG/DTG curve of gangue can be obtained as a function of the heating rate; i.e., the TG curve reflects the rule of change of the gangue body affected by temperature in the process of procedural warming, while the DTG curve is obtained by solving the first-order derivative of the TG curve, which reflects the rule of change of the mass change rate of the thermal mass loss of the gangue with the temperature in the process of gangue reaction.

3.1.1. Analysis of the TG/DTG Curve during the Pyrolysis of CG. Tests on the pyrolysis characteristics of gangue and raw coal in a nitrogen atmosphere were conducted, and the latent parameters are all reflected by the trends of TG/DTG curves,[26] including the following:

1 Curve peak temperature T_p, $T_{pmax;}$
2 Peak corresponding to the release rate of DTG curve volatiles $(dw/dt)_p$, $(dw/dt)_{pmax}$, %/s.

As shown in Figure 1a,b, the trends of TG/DTG curves of gangue and raw coal pyrolysis process under nitrogen conditions are basically similar, and the TG/DTG heat loss curve with a 5 °C/min heating rate was taken as an example to analyze the change characteristics of different temperature stages in the pyrolysis process of CG. From Figure 1a, it is observed that along with the increase of gangue temperature, there are obvious heat loss changes in different reaction stages, which can be mainly divided into the dry degassing stage, the active thermal decomposition stage, and the thermal

https://doi.org/10.1021/acsomega.3c09743
ACS Omega 2024, 9, 14174−14186

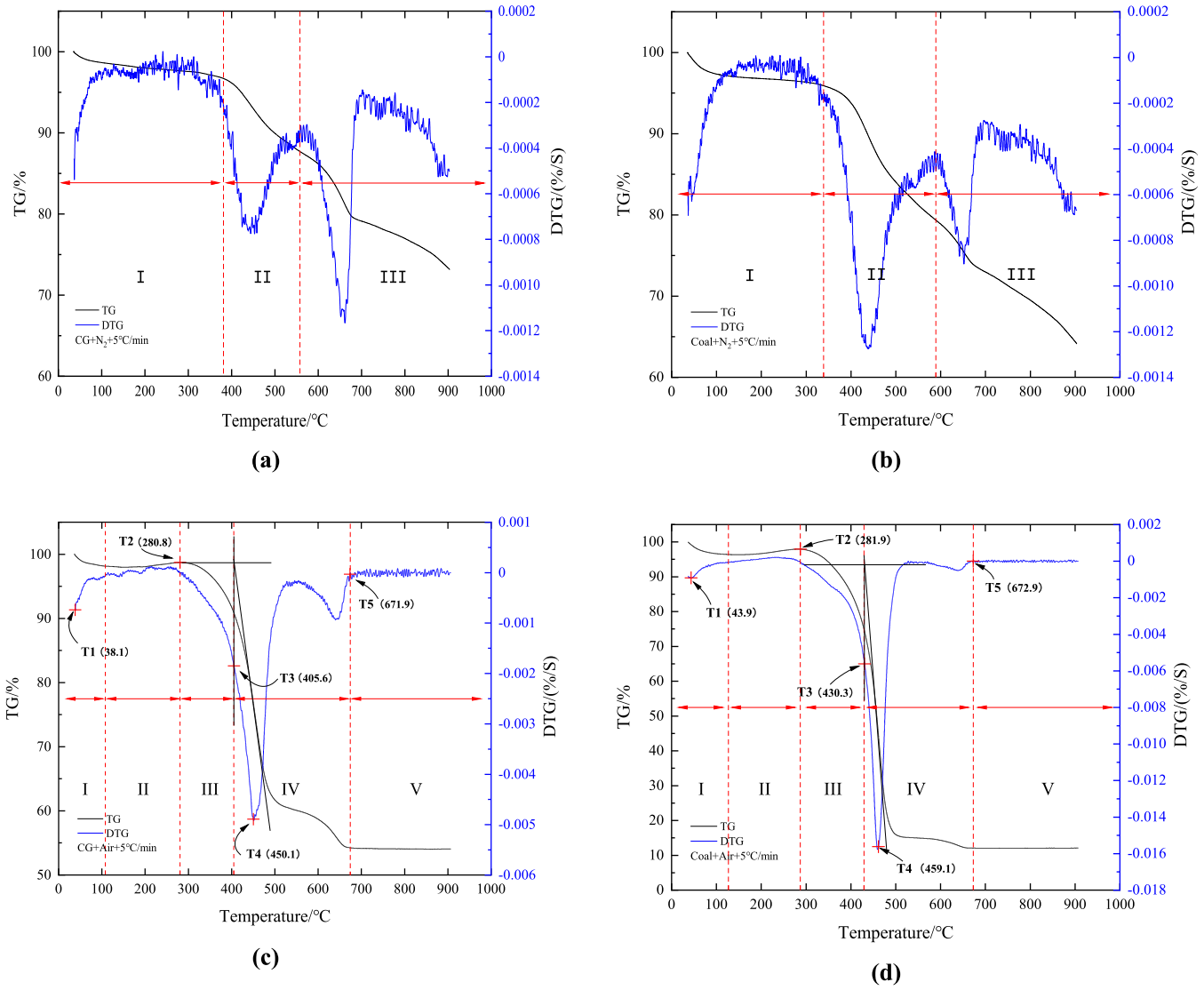

Figure 1. TG/DTG curves of coal/CG during pyrolysis at different heating rates in a N_2/air atmosphere: (a) TG/DTG curve of CG in the pyrolysis process of a N_2 atmosphere (β = 5 °C/min), (b) TG/DTG curve of coal in the pyrolysis process of a N_2 atmosphere (β = 5 °C/min), (c) TG/DTG curve of CG in the air atmosphere oxidation process (β = 5 °C/min), and (d) TG/DTG curve of coal in the air atmosphere oxidation process (β = 5 °C/min).

condensation stage.[26] In the dry degassing stage (stage I), with the temperature ranging from 35 to 380 °C, the TG curve slowly and linearly decreases, and the weight loss of the gangue is 3.25%, whereas there exists a DTG curve with a weak trough. While the DTG curve exhibits a weak trough, which is caused by the removal of surface and pore-bound moisture in CG before 120°C, followed by the gradual desorption of adsorbed gases (including CO, CO2, and CH4) as well as the removal of some small molecular substances embedded in the molecular structure of CG. active thermal decomposition stage (stage II), the temperature range of 380 °C ∼ 558 °C, the TG curve shows a straight-line downward trend, weight loss of up to 9.04%, especially in the DTG curve weight loss peak at 446 °C weight loss rate is very obvious, this process, the gangue original macromolecular structure began to crack, depolymerization, as well as the occurrence of some of the internal condensation reaction, a large number of volatiles of the escape, such as gas, coal tar, carbon oxides and moisture; thermal condensation stage (stage III), the temperature range of 558 °C ∼ 900 °C, the DTG curve appearing. The second weight loss peak (that is, the gangue secondary reaction) reached its maximum value this time with a weight loss rate of 6.46% at 661 °C ; this stage mainly involves the intermolecular polycondensation reaction, with the primary occurrence of a cross-linking bond rupture and at the same time the release of hydrocarbons, hydrogen, heterocyclic compounds, and carbon oxides, along with pyrolysis of water and other substances; some highly reactive volatile components escaped during the process of cleavage and polymerization again and the secondary reaction. The secondary reaction occurs, and the weight loss peak of the secondary reaction is narrower than that of the thermal decomposition stage of the living wave; the weight loss rate is high, due to which the residual solid is slowly aromatized.[13,16,17,19]

3.1.2. TG/DTG Curve Analysis of the Gangue Oxidation Process. Gangue is essentially a mineral with a low degree of metamorphism and potential for spontaneous combustion, similar to the trend of the TG/DTG curves during the increase in the coal oxidation temperature. Therefore, according to the literature,[27,28] the characteristic temperature in the TG/DTG

https://doi.org/10.1021/acsomega.3c09743
ACS Omega 2024, 9, 14174−14186

Table 3. Air Atmosphere Oxidation Rate of CG and Coal Is 5 °C/min, the Characteristic Temperature Point

name		T1	T2	T3	T4	T5
CG	temperature/°C	38.1	280.8	405.6	450.1	671.9
	mass/%	99.84	98.72	90.81	76.88	54.25
	DTG/(%/s)	-7.43023×10^{-4}	-3.34546×10^{-5}	−0.00185	−0.00489	-1.64736×10^{-4}
coal	temperature/°C	43.9	281.9	430.3	459.1	672.9
	mass/%	99.19	97.95	74.34	48.00	12.07
	DTG/(%/s)	-9.22828×10^{-4}	1.91898×10^{-6}	−0.00562	−0.01577	3.20132×10^{-6}

curve of CG during oxidative combustion is represented as follows: T1 is the critical temperature; T2 is the maximum point temperature of mass; T3 is the ignition temperature; T4 is the maximum thermal weight loss rate temperature point; and T5 is the burnout temperature. Figure 1c,d shows the TG/DTG curves of CG and coal during the oxidation in an air atmosphere, respectively. From the analysis, we learn what they look like at the characteristic temperature point during the oxidation autoignition. As shown in Table 3, the oxidative spontaneous combustion process of gangue can be divided into five stages,[29,30] i.e., water evaporation and degassing (phase I), oxygen absorption dynamiting (phase II), heating decomposition (phase III), combustion (phase IV), and burnout (phase V). The mass changes significantly at a disparate rate in different reaction phases, showing a specific law.

The TG/DTG curve of CG when slowly oxidizing and heating in the air atmosphere can completely reflect how the mass of CG changes from the initial temperature when it is oxidized by the air to the ignition temperature until the combustion is over and complete and how its mass loss rate changes during the compound oxidation reaction. The reaction processes in various phases are as follows:

(1) Phase I: this phase includes water evaporation and degassing; from the initial temperature of 36.5 °C to the dry cracking temperature of 113.6 °C, the gangue TG curve slowly bends downward, and the mass loss is 1.85%. At this stage, the moisture on the surface of the gangue and some of the gases adsorbed by the micropore (such as CO, CH_4, and N_2) are analyzed. At the critical temperature of 38.1 °C, the reaction rate gets faster and so does the binding rate of the active structure with the oxygen. Chemical reactions occur, releasing more CO, CO_2, and other gases.

(2) Phase II: this phase includes oxygen absorption and weight gain; between the dry cracking temperature point 113.6 °C and the mass maximum temperature point 280.8 °C (T2), the TG curve reaches a brief balance and then slowly rises to the extreme point; the CG has mass gain of 0.6% after oxygen absorption. After the dry cracking temperature point, the chemical oxygen adsorption and the gas desorption of CG will have a transient dynamic balance, resulting in a short-term stability in its mass, and then the dynamic equilibrium is disrupted. The number of reactive groups in the gangue increases rapidly with increasing temperature; the oxidation reaction runs at a faster rate; the oxygen uptake shoots up; and macroscopically, the mass of CG builds up.

(3) Phase III: this phase includes thermal decomposition; from the mass maximum point temperature 280.8 °C (T2) to the ignition temperature 405.6 °C (T3), the TG/DTG curve shows a rapid downward trend; the CG loses 7.91% mass at a rate of about −0.00185%/s ∼ -3.34546×10^{-5}%/s; the gangue mass starts to swoop in this phase; and rapid oxidative decomposition of the gangue's aromatic ring structure generates large quantities of CO and CO_2 gases as well as small-molecule organic gases. The volatiles also burn slowly, gradually increasing the heat release, and aggregate to reach the ignition temperature of CG.

(4) Phase IV: this phase includes combustion; from the ignition temperature (T3) 405.6 °C to the burnout temperature point (T5) 671.9 °C, the TG curve takes a nose dive at the maximum peak temperature 450.1 °C (T4), and then a small amplitude of reaction peak appears, which then plummets at the secondary reaction peak temperature of 644.5 °C, until reaching the burnout temperature T5, while the DTG curve shows a maximum thermal mass loss rate at T4. The weight loss between T3 and T4 reaches 13.93%, and that between T4 and T5 is 22.63%, with the total weight loss being 36.56%. The maximum weight loss rate reaches −0.00489%/s, with the maximum weight loss rate at the secondary reaction peak being -9.05912×10^{-4}%/s. In this phase, the active molecular structure of CG generates a strong chemical reaction with the oxygen to cause the molecular chain to break, the mass drastically decreases, and the oxygen consumption increases sharply, while the DTG curve has two distinct peaks characteristic of the volatile analyzed combustion phase and the stationary charcoal combustion phase.[31] The first mass loss peak is the maximum, long and narrow in shape; the second mass loss peak is smaller than the first, which shows that the chemical reaction of the maximum peak volatiles is the most intense and consumes more oxygen at the fastest rate; the second peak is the maximum heat mass loss point for the combustion of fixed carbon, until the fixed carbon completely burns out.

(5) Phase V: this phase involves burnout; from the burnout temperature of 671.9 °C to the finishing temperature of 900 °C, the TG curve is stable at around 54.25%, while the DTG curve has a mass loss rate of -1.764736×10^{-5}% at the burnout temperature, which also tends to be zero. The total mass loss from the initial temperature of 36.5 °C to the burnout temperature is 45.72%, which suggests that the combustible material in the CG after the burnout temperature has been completely burned out; the remaining minerals have not yet been decomposed, and the mass does not significantly increase or decrease.

3.2. Analysis of Thermogravimetric Curve Characteristics of CG at Different Heating Rates. CG is a complex mixture, and its spontaneous combustion reaction process is affected by a variety of factors, such as different source types, heating rate, particle size, and the pressure of the surrounding

https://doi.org/10.1021/acsomega.3c09743
ACS Omega 2024, 9, 14174−14186

Table 4. Pyrolysis Peak Characteristic Parameters of CG in a Nitrogen Atmosphere at Different Heating Rates

ramp rate/(°C/min)	initial temp	dw/dt/(%/s)	T_p/°C	$(dw/dt)_p$/(%/s)	T_{pmax}/°C	$(dw/dt)_{pmax}$/(%/s)
5	35.4	-4.48927×10^{-4}	444.1	-7.74989×10^{-4}	661.3	−0.00117
10	35.3	-8.27827×10^{-5}	455.2	-7.27156×10^{-4}	679.6	−0.00105
20	35.5	-2.72916×10^{-4}	464.6	-7.99908×10^{-4}	697.5	-9.71096×10^{-4}
30	35.5	-1.68222×10^{-4}	470.3	-7.63239×10^{-4}	710.8	-9.23057×10^{-4}

gas, atmosphere, temperature, time, etc.[32−36] Meanwhile, this paper focuses on exploring the reaction law of gangue in nitrogen and air atmosphere pyrolysis as well as oxidative combustion process impacted by the rate of heating, aiming to derive the degree of influence of gangue by oxygen and the rate of heating in different phases, the trend of change, and to study the differences and similarities of its overall law.

3.2.1. Pyrolysis Characteristic Curves of CG at Different Heating Rates in a Nitrogen Atmosphere. As shown in Table 4 and Figure 2, the pyrolysis characteristic curves of gangue

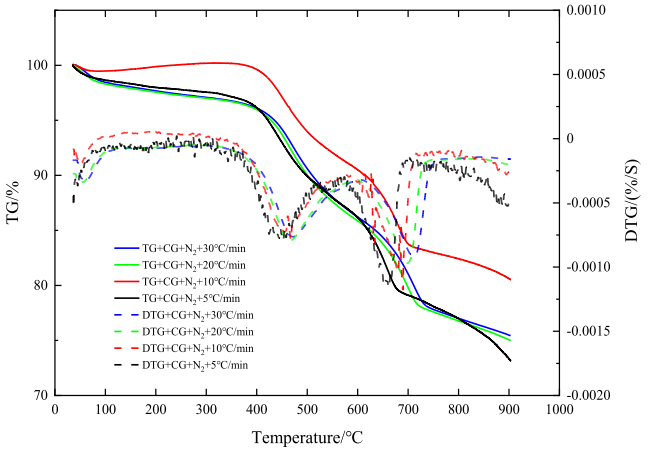

Figure 2. Pyrolysis characteristic curve of CG in a N_2 atmosphere at different heating rates.

under a nitrogen atmosphere at different heating rates have basically similar trends at each stage. The trends of the TG curves for heating rates of 5, 20, and 30 °C/min were basically in agreement, while at the heating rate of 10 °C/min, the mass loss in the whole pyrolysis process is more moderate than other curves, and at 600−700 °C next to the maximum peak of mass loss, the curve is out of shape, which may be attributed to insufficient reaction of CG or detector fault; the extreme thermal mass loss peak $(dw/dt)_p$ of the DTG curve shows a similar value at 400−500 °C with an increase in the pyrolysis rate, but the maximum thermal mass loss peak $(dw/dt)_{pmax}$ gradually slopes down in the range of 600−750 °C; the pyrolysis mass loss peak temperature is biased toward the high-temperature zone[13,17,19] since CG has a poor thermal conductivity due to "high ash content and low carbon content", and with the increase of heating rate, uneven temperature rise in the CG molecules leads to an increased temperature difference between the inside and the outside at an increasing heating rate; in this case, the external pyrolysis product is not diffused timely, and thermal hysteresis occurs; while its internal temperature is relatively low, the lower pyrolysis rate leads to a delay in the volatilization process, so that the pyrolysis peak shifts to the higher-temperature zone.

3.2.2. Characteristic Curves of Oxidative Combustion of Gangue under an Air Atmosphere at Different Heating Rates. Figure 3 shows the TG/DTG curves of oxidative combustion of gangue in an air atmosphere at different heating

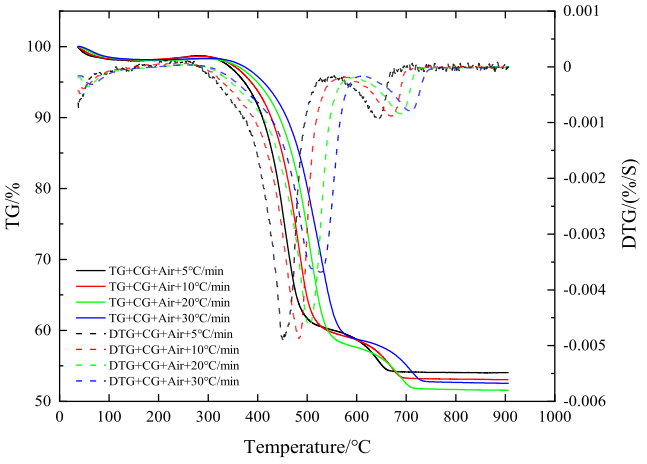

Figure 3. Oxidation characteristic curve of CG in an air atmosphere at different heating rates.

rates. The whole heating process is characterized by staged characteristics, and the curves of different heating rates contain five phases of oxidative combustion characteristics stage, and the characteristics of the various stages vary considerably. Two thermogravimetric peaks appear in the combustion process in the DTG curve, of which one has a maximum thermal loss rate long and narrow in shape and the other has a relatively low mass loss rate. With the increase of the heating rate, at two mass loss peaks, the temperatures shift toward the high-temperature areas, and it can be seen that the heating rate has a great influence on the combustion stage of CG. Figure 3 shows the oxidation characteristic curve of different air atmospheres of gangue at different heating rates, and Table 5 shows oxidation combustion characteristic parameters of gangue at different heating rates.

As can be seen from Figure 3 and Table 5, with the increase of the gangue heating rate, the characteristic temperature at different temperature stages presents a linear increase trend, and the peak temperature of the DTG curve moves to the high-temperature region; the peak heat loss rate shows a gradual decrease trend, indicating a hysteresis phenomenon. At the same time, when the heating rate is large, the heat released by the reaction has difficulty in supporting the response of the burning components, indicating that the heat loss rate slows down with the increase of the system temperature. During the oxidative heating process of CG, the thermal loss in the phase I water evaporation and degassing falls within 1.66−1.85%, 0.03−0.6% in phase II oxygen absorption dynamiting, 7.91−10.02% in phase III heating decomposition, and 35.28−36.73% in phase IV combustion, and the mass loss in phase V burnout almost approaches zero; the total thermal mass loss in the whole combustion process is 46.32−47.95%, accounting for 76% of the total mass loss; the content of remnants is 51.75−

https://doi.org/10.1021/acsomega.3c09743
ACS Omega 2024, 9, 14174−14186

Table 5. Characteristic Parameters of Oxidation Combustion under Different Heating Rates of CG[a]

name	heating rate/°C/min			
	5	10	20	30
T1	38.1	36.4	57.4	65.1
T2	280.8	287.5	299.5	301.7
T3	405.6	434.6	453.9	460.3
T4	450.1	481	503.6	524.2
T5	671.9	696.7	709.4	729.3
I mass/%	−1.85	−1.78	−1.69	−1.66
II mass/%	+0.6	+0.43	+0.03	+0.04
III mass/%	−7.91	−10.02	−10.01	−8.63
IV mass/%	−36.56	−35.28	−36.25	−36.73
V mass/%				
total loss of mass/%	−46.32	−47.08	−47.95	−47.02

[a]Note: "−" represents the mass loss; "+" represents the mass gain.

53.28%. Figure 3 shows that CG contains volatiles, fixed carbon, and other flammable substances in this phase, and the combustion is relatively sufficient, until there is no more flammable substance to react in the burnout phase.

3.3. Comparative Analysis of the Thermogravimetric Curves of CG and Raw Coal.

3.3.1. TG/DTG Pyrolysis Curve. As shown in Figure 4, the pyrolysis curves of CG and

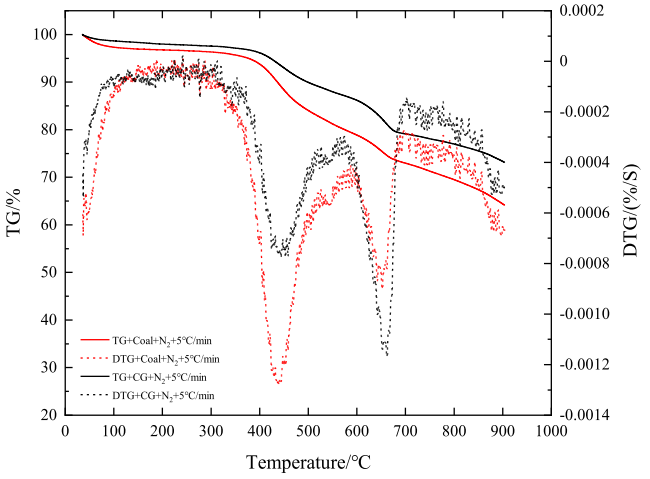

Figure 4. Pyrolysis characteristic curve of coal/CG in a N_2 atmosphere.

raw coal are given under a nitrogen atmosphere. The pyrolysis characteristic curves of raw coal and CG at a heating rate of 5 °C/min are chosen for comparative analysis. From Figure 4, it can be seen that the entire pyrolysis process of raw coal and CG is similar, with a total weight loss of 35.83% during the entire heating pyrolysis process, which is 9% higher than that of CG. DTG also has two mass loss peaks; one in the active wave thermal decomposition phase is narrower and higher than that of CG and the other at the secondary reaction of the thermal polycondensation phase is the other way; this may be attributed to the higher volatiles and fixed carbon content but the lower ash content in the coal. During the active pyrolysis phase, more active functional groups generate, resulting in intense reactions, whereas in the thermal condensation phase, the content of volatile gases released from condensation reactions reduces. As a result, the pyrolysis reaction processes of coal and gangue in these two stages differ very significantly.

3.3.2. Characteristic Curves of TG/DTG Oxidation Combustion of CG and Raw Coal. As shown in Figure 5,

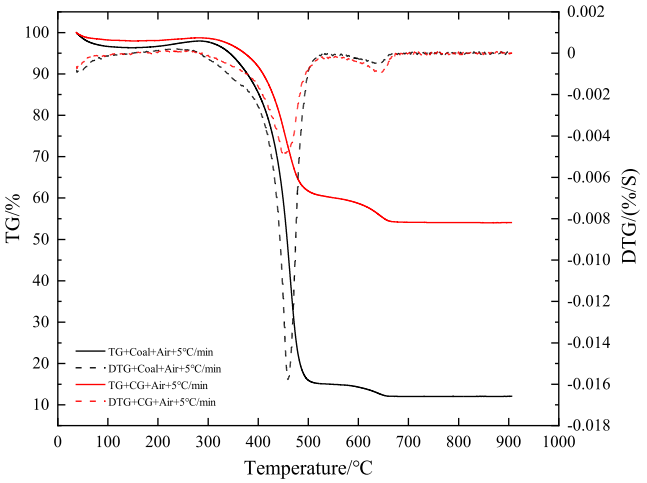

Figure 5. Characteristic curve of oxidation and combustion of coal/CG in an air atmosphere.

there are the TG/DTG curves of CG and raw coal in the oxidative combustion in air; Table 6 shows the appropriate latent parameters for the two in this process. It can be concluded from them that the phased behaviors presented by the coal in the heating process are similar to those by the gangue. The mass loss of coal in phases I, III, and IV is 1.65, 15.7, and 25.74% higher than that of gangue, respectively, which suggests that reactions of coal in these three phases seem more intense. In particular, it is known from the DTG curve that there are two thermal mass loss peaks in the thermal decomposition and combustion phases, which may be due to the decomposition and combustion of volatiles and fixed carbon. From the proximate analysis, it is found that the total content of volatiles and fixed carbon in the coal accounts for 82.78, 37.54% higher than that in CG; it is also true in phase II oxygen absorption dynamiting, 0.88% higher than that in CG. It may be attributed to more active functional groups and types that absorb more oxygen in the coal structure; the mass losses of coal and gangue are basically zero in the burnout phase, but the remnant of coal is 12.07, 33.65% less than that of gangue. This is because the ash content in CG is higher and the substances involved in the reaction are rare. If the temperature continues to rise, then the remnant will also have a secondary reaction. As observed from the DTG curves of coal and CG, the difference between the characteristic temperatures before the ignition temperature T3 is less, and the difference between the ignition temperature point T3 and the maximum heat loss rate temperature point T4 is large, which is primarily caused by the difference between the gangue and the coal decomposition and combustion stage of the volatile matter and fixed carbon content of the larger differences during the reaction process resulted from the different characteristics of the temperature differences.

3.4. Calculation of the Dynamic Parameters of CG.

CG not only has a similar molecular structure with coal but also has a similar spontaneous combustion process. The combustible substances in CG are slowly oxidized and self-heated when encountering oxygen, and the oxidation heat generation is greater than the environmental heat dissipation. The gradual accumulation of heat will lead to CGSC. In order

https://doi.org/10.1021/acsomega.3c09743
ACS Omega 2024, 9, 14174−14186

Table 6. Characteristic Parameters of Oxidation Combustion of Gangue and Coal[a] in an Air Atmosphere

name		T1/°C	T2/°C	T3/°C	T4/°C	T5/°C
CG	temperature/°C	38.1	280.8	405.6	450.1	671.9
	mass/%	99.84	98.72	90.81	76.88	54.25
	DTG/(%/s)	-7.43023×10^{-4}	-3.34546×10^{-5}	−0.00185	−0.00489	-1.64736×10^{-4}
coal	temperature/°C	43.9	281.9	430.3	459.1	672.9
	mass/%	99.19	97.95	74.34	48.00	12.07
	DTG/(%/s)	-9.22828×10^{-4}	1.91898×10^{-6}	−0.00562	−0.01577	3.20132×10^{-6}

weightlessness rate	I/%	II/%	III/%	IV/%	V/%	total weightlessness/%
CG	−1.85	+0.6	−7.91	−36.53	0	−46.29
coal	−3.5	+1.48	−23.61	−62.27	0	−89.38

[a]Note: "−" indicates the mass loss; "+" indicates the mass gain.

to better understand the reaction process in the process of CGSC, it is necessary to explore the reaction kinetics process of CG. The research on the kinetics of CG mainly focuses on solving the kinetic parameters[37,38] that characterize the reaction process during the CGSC, namely, the apparent activation energy E, pre-exponential factor A, and mechanism function $f(\alpha)$ or $G(\alpha)$ to reflect the difficulty of chemical reactions during coal spontaneous combustion and provide a theoretical basis for the early prevention of CGSC.

CG is a complex mixture, and using different methods to analyze the same thermogravimetric curve may also result in significant differences in the dynamic parameters solved. The kinetic analysis of gangue using the nonisothermal method can be mathematically divided into two categories: differential method and integral method; the operation mode contains two categories: the single scanning rate method and the multiple scanning rate method. The multiple scanning rate method, represented by the Flynn−Wall−Ozawa (FWO) method, the Kissinger−Akahira−Sunose (KAS) method, and the Friedman method,[39,40] represents a research method to analyze the kinetic process by experimentally obtaining several different TA curves at multiple heating rates. The multiple scan rate method is also called the "iso-conversional method" because it requires the use of data from several TA curves at the same conversion rate α. The iso-conversional method can be used to obtain highly reliable activation energy E values without solving the kinetic mechanism function of the reaction (also known as the model-free method), and it is still possible to analyze the activation energy E values against different conversions α to verify that the mechanism of the reaction is the same throughout the entire reaction process.

Starink[24,41,42] analyzed and compared the Kissinger equation, Ozawa equation, and Boswell equation. The general formula for the three equations is represented by (1), with C representing a constant in the four equations. The subscript S of constant C represents Starink.

$$\ln\left(\frac{\beta}{T^{s}}\right) = C_{S} - \frac{BE}{RT} \tag{1}$$

Based on the approximate solution of the temperature integral partial integral equation, the constants s and B in the equation are adjusted, and the Starink eq 2 for calculating the activation energy E is proposed

$$\ln\left(\frac{\beta}{T^{1.8}}\right) = C_{S} - \frac{BE}{RT} = C_{S} - 1.0037\frac{E}{RT} \tag{2}$$

Among them

$$B = 1.0070 - 1.2 \times 10^{-5}E\ (\mathrm{kJ \cdot mol^{-1}})$$
$$= 1.0070 - 1.2 \times 10^{-5} \times (66 \times 4.184) = 1.0037$$

The experiment confirms that the Starink equation has a greater advantage over other equations when solving the activation energy E; at the same time, Yang Fuqiang[42] used five thermal analysis methods, including Coats Redfern equation, Flynn Wall Ozawa equation, Kissinger equation, Starink equation, and Friedman equation, to calculate the activation energy of coal thermal decomposition reaction, which also verified the better effect of the Starink method.

This section uses the Starink method in the multiple scanning rate method to study and analyze the thermogravimetric curves of CG samples with heating rates of 5, 10, 20, and 30 °C/min under air atmosphere conditions[41] and calculates the TG curves of different heating rates at the same conversion rate α the values of "$\ln(\beta/T^2)$" and "$1.0037/RT$" below, analyze and plot and perform linear fitting. The slope of the linear fitting equation is $-E$, which represents the "apparent activation energy of CG". Figure 6 shows the different heating rates of gangue conversion rate α and temperature T rule of change, indicating that the change trend is consistent at different heating rates of gangue with the increase in the temperature conversion rate; the trend shows a "slow first, then fast, and gradually slows down" pattern, ultimately approaching 1; however, the general trend of the

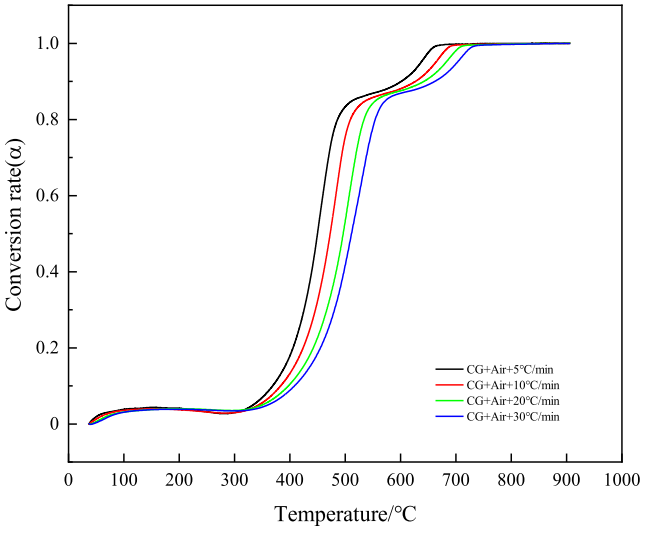

Figure 6. Relationship curve between the CG conversion rate (α) and temperature.

https://doi.org/10.1021/acsomega.3c09743
ACS Omega 2024, 9, 14174−14186

curve shifts toward the high-temperature region as the heating rate increases; prior to 300 °C, the temperature point values for different heating rates are essentially equal at the same conversion rate. After 300 °C, the temperature points for different heating rates to reach the same conversion rate also increase with the increase of heating rate. This indicates that the increase of the heating rate does not change the efficiency of the conversion rate but only promotes the hysteresis of the gangue reaction temperature.[25]

For the apparent activation energy of the gangue oxidative autoignition process, the data of TG curves at different heating rates under the same conversion rate α were selected at intervals of 0.05 each. The data for Starink equations $\ln(\beta/T^2)$ and $1/RT$ were obtained, and a diagram was drawn, as shown in Figure 7; the results obtained from linear fitting are shown

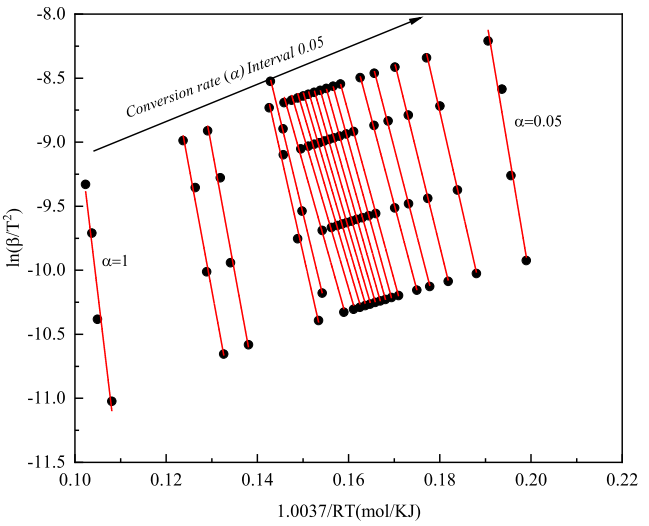

Figure 7. Linear fitting relationship between $\ln\frac{\beta}{T^2}$ and $\frac{1}{RT}$ of CG under different conversion rates (α) in an air atmosphere.

in Table 7. From Figure 7, it can be seen that the slope of the linear fitting equation for CG with a conversion rate between 0.8 and 1 gradually increases, and the intercept also increases accordingly; between 0 and 0.8 conversion rates, the slope of the linear fitting equation gradually decreases, and the longitudinal intercept also decreases accordingly; the fitting accuracy R^2 of the linear equation in Table 7 kinetic parameters of CG is more than 0.98, which can also confirm that the credibility of the apparent activation energy of CG solved by the Starink equation is high.[43]

Figure 8 shows the real-time shift of the conversion rate of the gangue oxidation process in relation to the apparent activation energy; the activation energy in the gangue oxidation combustion process into the high conversion rate of 80−100% stage shows a rapid growth trend. At this time, the CG has passed the maximum heat loss point temperature T4, and the volatile components of the CG have been completely burned, entering the fast oxidation combustion stage of fixed carbon until the end of the combustion stage, with the conversion rate before 80%. On the whole, the activation energy gradually decreases, with a rapid decrease between 0 and 40%. CG is in the slow combustion stage before thermal decomposition to the maximum thermal weight loss, and the change range between 40 and 80% is very small; the gangue is in the temperature range where the heat weight loss is the greatest. In

Table 7. Kinetic Parameters of CG Oxidation and Spontaneous Combustion

α	linear fitting equation	E/(kJ/mol)	R^2
0.05	$y = -211.40x + 32.168$	211.40	0.9725
0.10	$y = -156.29x + 19.371$	156.29	0.9974
0.15	$y = -144.79x + 16.249$	144.79	0.9992
0.20	$y = -137.67x + 14.360$	137.67	0.9994
0.25	$y = -134.25x + 13.337$	134.25	0.9995
0.30	$y = -147.19x + 12.521$	147.19	0.9995
0.35	$y = -130.11x + 12.044$	130.11	0.9999
0.40	$y = -129.06x + 11.648$	129.06	1.0000
0.45	$y = -127.03x + 11.124$	127.03	1.0000
0.50	$y = -124.99x + 10.629$	124.99	1.0000
0.55	$y = -123.51x + 10.236$	123.51	0.9995
0.60	$y = -121.85x + 9.8226$	121.85	0.9990
0.65	$y = -121.23x + 9.5801$	121.23	0.9985
0.70	$y = -120.73x + 9.3517$	120.73	0.9974
0.75	$y = -120.83x + 9.1925$	120.83	0.9966
0.80	$y = -126.38x + 9.7898$	126.38	0.9964
0.85	$y = -157.94x + 13.826$	157.94	0.9920
0.90	$y = -193.46x + 16.107$	193.46	0.9820
0.95	$y = -192.45x + 14.864$	192.45	0.9894
1.00	$y = -298.29x + 21.144$	298.29	0.9619

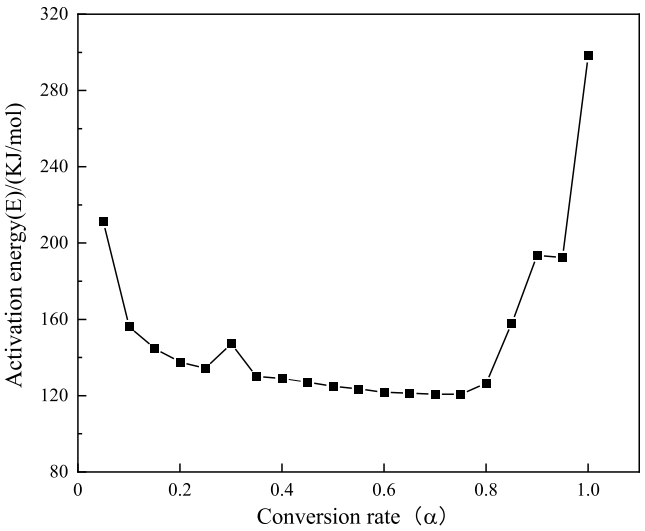

Figure 8. Real-time conversion law of activation energy during the CG oxidation combustion process.

the process of oxidizing combustion of CG, the conversion values of water evaporation, gas desorption stage, and oxygen absorption weight gain stage are very small, so the activation energy selected data cannot reflect the reaction and function of these two stages, while for the thermal decomposition of gangue and part of the volatile components of the combustion stage, the apparent activation energy is in a rapidly decreasing trend, with a consistent reaction mechanism function. For the combustion stage of the thermal decomposition and partial volatile matter of CG, the apparent activation energy shows a fast-decreasing trend and exerts a consistent reaction mechanism function. The apparent activation energy changes very little around the maximum temperature of thermal weight loss in CG. After that the apparent activation energy continues to increase, indicating that the maximum temperature point of the heat loss is, in the entire combustion process, in a

https://doi.org/10.1021/acsomega.3c09743
ACS Omega 2024, 9, 14174−14186

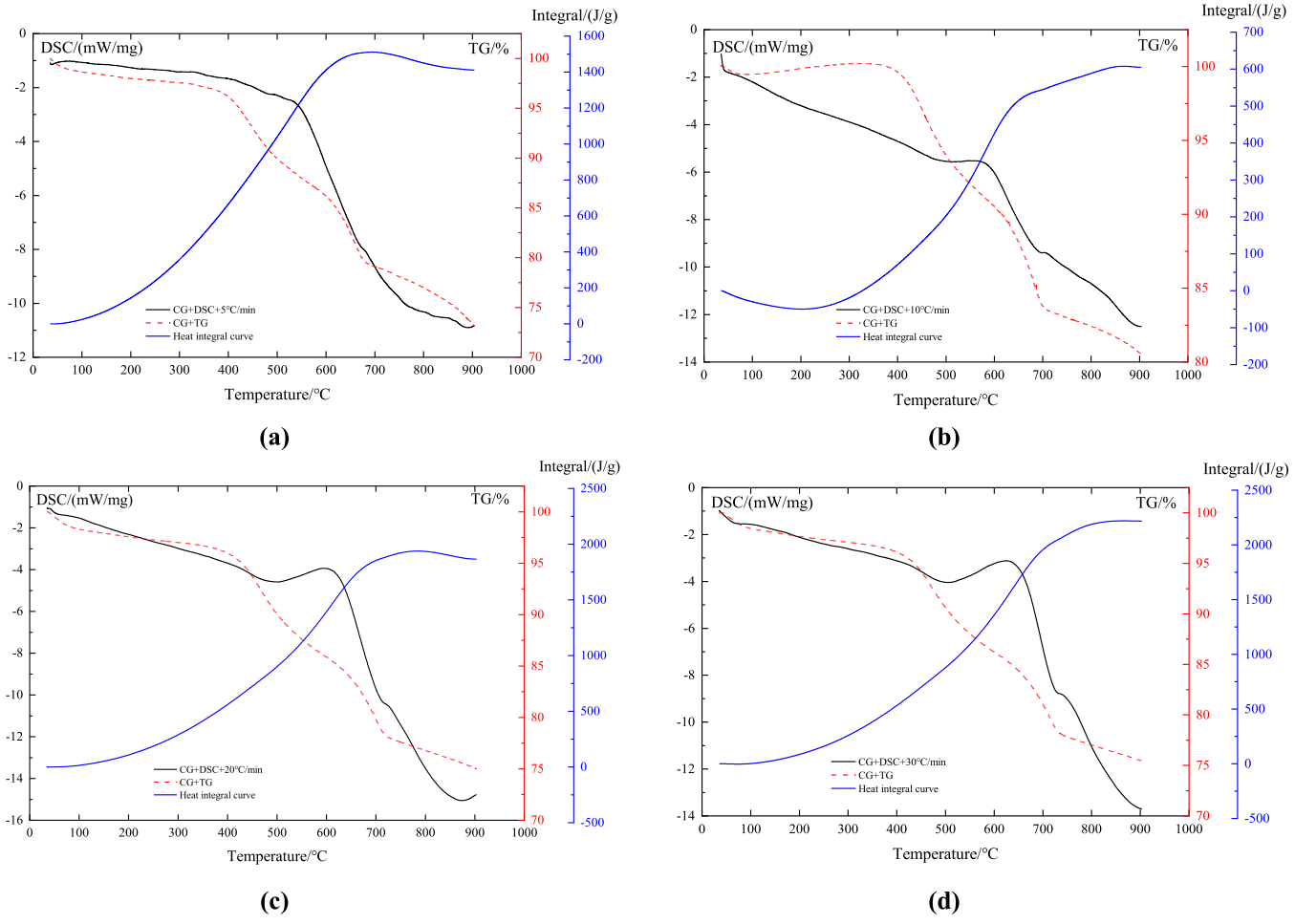

Figure 9. DSC curves of CG in a N_2 atmosphere at different heating rates: (a) DSC curve with a heating rate of 5 °C/min, (b) DSC curve with a heating rate of 10 °C/min, (c) DSC curve with a heating rate of 20 °C/min, and (d) DSC curve with a heating rate of 30 °C/min.

transitional stage of the reaction mechanism function, which is also a difference.[44]

3.5. Study on the Thermal Effect of the CG Reaction Process. The CG spontaneous combustion reaction process involves the interaction of gangue with oxygen and leads to the gangue being gradually slowly oxidized,[24,45] the reaction of the release of heat continues to accumulate to promote oxidation rate intensification, and the accumulation of heat to reach the critical point of spontaneous combustion gangue leads to spontaneous combustion. Thermal analysis experiment can accurately test the process of heat production of CG in real time, so as to better study the exothermic properties of CG in the process of spontaneous combustion and to gain more insight into the mechanism of the self-heating process of gangue.[8]

The synchronous thermal analysis experiment conducted synchronous testing on CG samples in 2 atm of air and nitrogen as well as at different heating rates. The DSC curve corresponding to the TG curve was obtained, which can reflect the transformation process of the heat flux difference between the sample and the reference material during the heating process of the CG sample. The DSC curves of CG temperature rise at different heating rates were integrated to obtain patterns of heat and temperature changes. The slope of the integration curve is the heat release rate, which is positively correlated with the heat flux difference of the gas DSC curve. The DSC curves and integration curves of samples at different heating rates and in different gas atmospheres are shown in Figures 9 and 10. The peak pattern shows the exothermic direction upward and the endothermic direction downward.[20]

From Figure 9, it can be seen that the DSC curve of the pyrolysis process of gangue in a nitrogen atmosphere presents the characteristics of first slow and then fast. The overall pyrolysis process is in the endothermic stage, corresponding to a maximum endothermic peak during the transition from the active wave thermal decomposition stage to the thermal condensation stage of the TG curve, where the reaction endothermic rate reaches its maximum value; with the continuous improvement of the pyrolysis heating rate, this transition section will shift toward the thermal condensation stage, and the peak value will gradually increase. At the same time, the heat curve will also rapidly grow and reach a maximum value.[46]

Based on Figure 10, it can be observed that the change in heat during the entire oxidation heating process of CG is mainly caused by the phases of heat absorption from moisture evaporation and gas desorption, weight gain from oxygen absorption, and combustion of fixed carbon, as well as the phases of heat release from active pyrolysis and combustion of volatile matter. Along with the growth of oxidation heating rate, the exothermic stage of the peak area is getting bigger and bigger, the heat integral curve here also undergoes a sudden change from exothermic to adsorption, and the heat integral curve is also changed to adsorption by exothermic, the

https://doi.org/10.1021/acsomega.3c09743
ACS Omega 2024, 9, 14174−14186

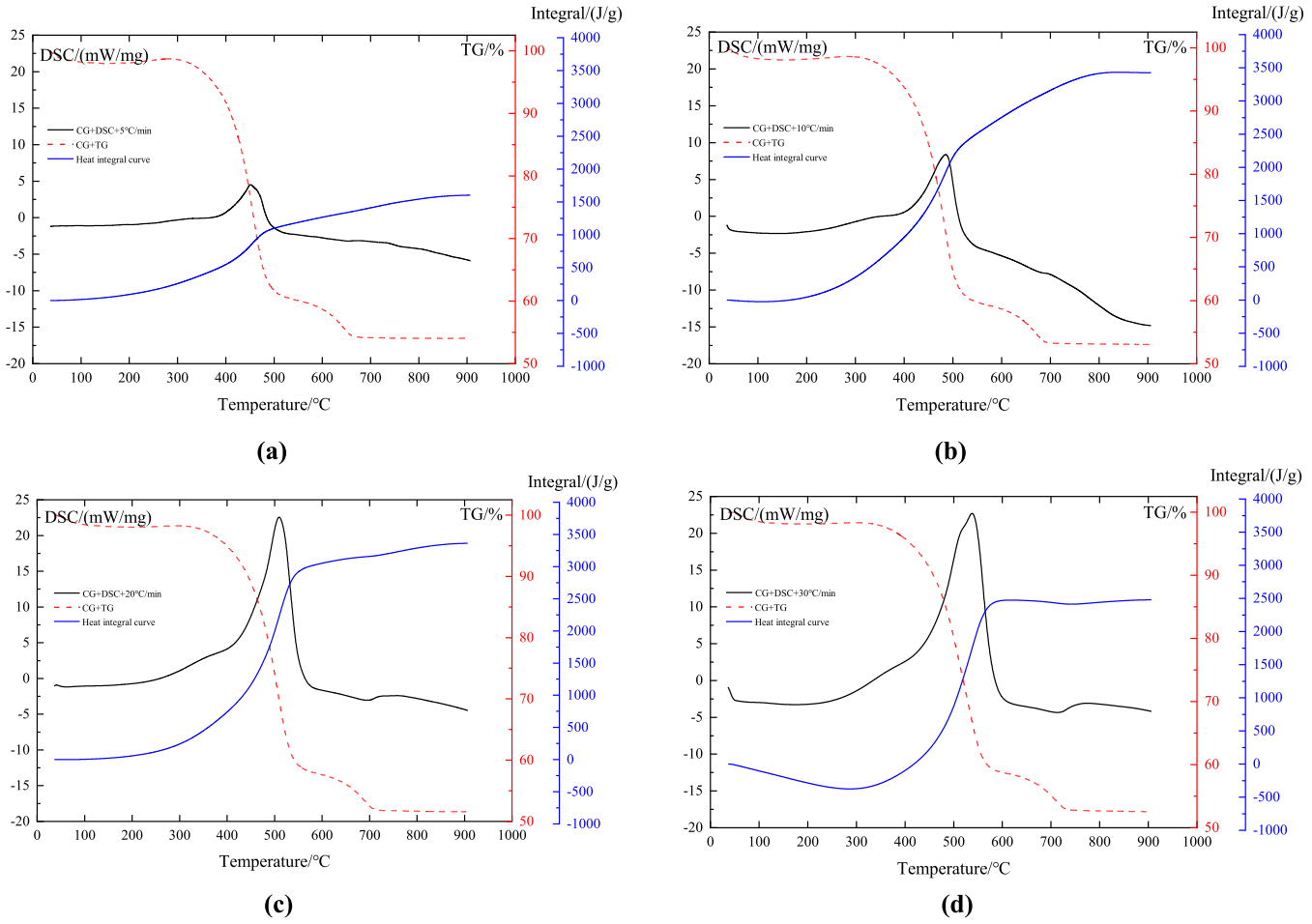

Figure 10. DSC curves of CG in an air atmosphere at different heating rates: (a) DSC curve with a heating rate of 5 °C/min, (b) DSC curve with a heating rate of 10 °C/min, (c) DSC curve with a heating rate of 20 °C/min, and (d) DSC curve with a heating rate of 30 °C/min.

endothermic reaction rate decreases, and the exothermic stage also shifts toward a higher temperature range as a whole.

As can be seen from Figure 11, the overall pyrolysis process of CG has always been in the endothermic stage, while there is a partial exothermic stage in the spontaneous combustion process. With the increase of the heating rate of CG, the DSC curves of CG pyrolysis and oxidation combustion both have a "lag" phenomenon that shifts toward high temperature.[47] This may be because the physical property parameters of CG determine that the higher heating rate does not directly lead to acceleration of the reaction, but passive heating leads to hysteresis of the thermal effect. Therefore, it is important to select the appropriate heating rate for analysis of the reaction process.

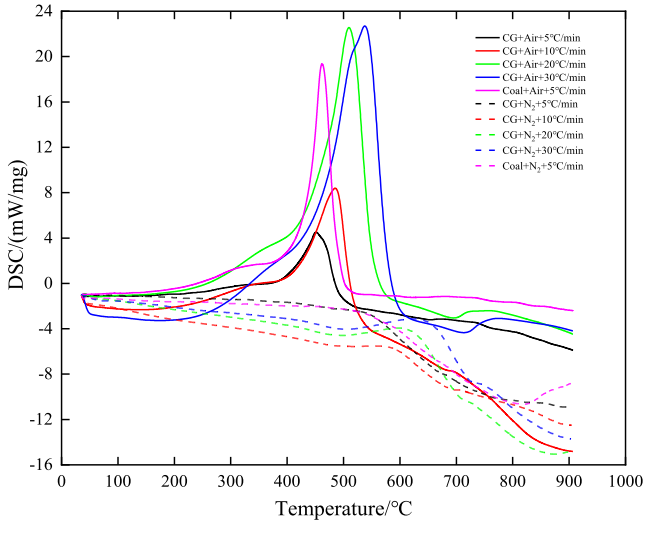

Figure 11. DSC curves of CG/coal at different heating rates.

4. CONCLUSIONS

This study uses TGA-DSC combined thermal analysis technology to test samples with different heating rates during CG pyrolysis and oxidation combustion processes. At the same time, the reaction kinetic parameters and heat release characteristics of CG are studied, and the variation law of the reaction kinetics process of CG is obtained:

(1) Thermogravimetric analysis revealed the pyrolysis and oxidation process of CG, and the stages of the CG thermogravimetric curve under different gas atmospheres were significantly different. The whole pyrolysis process is mainly divided into the dry degassing stage, the active thermal decomposition stage, and the thermal condensation stage. The oxidation−combustion process can be divided into five parts: water evaporation and gas desorption stage, oxygen absorption weight gain stage, thermal decomposition stage, combustion stage, and

https://doi.org/10.1021/acsomega.3c09743
ACS Omega 2024, 9, 14174−14186

burnout stage. The establishment of characteristic temperature points provides a basis for accurately dividing the spontaneous combustion stage of gas and establishing an early warning system.

(2) Compared with raw coal, the thermogravimetric curve of pyrolysis and oxidative combustion process of raw coal show the same phase change trend as that of CG, except that the difference in the amplitude change of different phase peaks is more obvious, so it can be studied by drawing on the mature research method, monitoring and prevention technology, and other related theoretical systems and engineering technologies of coal spontaneous combustion, and in-depth study of CGSC will also help to improve the development of the research process of coal spontaneous combustion.

(3) The Starink equation in the multiscan rate method was used to analyze the activation energy of the entire oxidation reaction process of CG; the fitting accuracy R^2 of linear equations exceeds 0.98. In the high conversion stage ($\alpha > 80\%$), the activation energy showed a trend of rapid growth, and CG was in the oxidation and combustion stage of fixed carbon, while in the low conversion stage ($\alpha < 80\%$), the activation energy showed a trend of rapid rise followed by a slow decline. CG is in a slow burning phase before being decomposed by heat to maximum loss of focus. Based on this, CGSC can be accurately and efficiently prevented by increasing the activation energy of CG at different oxidation combustion stages by using inhibitors with the corresponding inhibition rates at different stages.

(4) The DSC curve of CG pyrolysis shows a decreasing trend, showing a process of heat absorption. The DSC curve of oxidation combustion process has a large heat release peak in the thermal decomposition stage and the combustion stage, and the other stages are also in the state of oxidation heat absorption. Therefore, it is necessary to effectively prevent and control the oxidation heat storage process of CG before these two stages to avoid the CGSC.

(5) With the increase of temperature, the CG conversion rate of different heating rates showed a consistent trend, showing a trend of "first slow, then fast, and then gradually slow" and finally close to 1. An increase in the heating rate only causes a "lag" at the characteristic temperature point and does not change the efficiency of the conversion. Therefore, it is necessary to study the temperature fields on the surface and inside of gangue hills that have not been or have been stored for heat in the early stages and take control measures such as heat transfer, isolation, monitoring, and inhibition in a hierarchical and coordinated manner to reduce the heating rate inside and outside the gangue mountain and avoid CGSC. In addition, the "lag" of characteristic temperature points also means that the early warning and prevention work of hidden dangers of CGSC has more time to respond to and deal with these issues.

AUTHOR INFORMATION

Corresponding Author

Dailin Li − *College of Safety Science and Engineering, Xi'an University of Science and Technology, Xi'an 710054, China;* orcid.org/0009-0007-5113-4243; Email: 790167611@qq.com

Authors

Yongfei Jin − *College of Safety Science and Engineering, Xi'an University of Science and Technology, Xi'an 710054, China; Key Laboratory of Western Mine and Hazard Prevention, Ministry of Education of China, Xi'an 710054, China; Shaanxi Key Laboratory of Prevention and Control of Coal Fire, Xi'an 710054, China*

Yin Liu − *College of Safety Science and Engineering, Xi'an University of Science and Technology, Xi'an 710054, China; Key Laboratory of Western Mine and Hazard Prevention, Ministry of Education of China, Xi'an 710054, China; Shaanxi Key Laboratory of Prevention and Control of Coal Fire, Xi'an 710054, China*

Jun Guo − *College of Safety Science and Engineering, Xi'an University of Science and Technology, Xi'an 710054, China; Key Laboratory of Western Mine and Hazard Prevention, Ministry of Education of China, Xi'an 710054, China; Shaanxi Key Laboratory of Prevention and Control of Coal Fire, Xi'an 710054, China*

Changming Chen − *College of Safety Science and Engineering, Xi'an University of Science and Technology, Xi'an 710054, China*

Xubin Yan − *College of Safety Science and Engineering, Xi'an University of Science and Technology, Xi'an 710054, China*

Complete contact information is available at: https://pubs.acs.org/10.1021/acsomega.3c09743

Notes

The authors declare no competing financial interest.

ACKNOWLEDGMENTS

This research was supported by the National Natural Science Foundation of China (grant nos. 52174198, 52004209, and 52304251).

ABBREVIATIONS

CG coal gangue
CGSC coal gangue spontaneous combustion
TG thermogravimetry
TGA thermogravimetry analysis
DTG differential thermal gravity
DSC differential scanning calorimetry

REFERENCES

(1) Cao, Z.; Cao, Y.; Dong, H.; Zhang, J.; Sun, C. Effect of calcination condition on the microstructure and pozzolanic activity of calcined coal gangue. *Int. J. Miner. Process.* **2016**, *146*, 23−28.

(2) Li, J.; Wang, J. Comprehensive utilization and environmental risks of coal gangue: a review. *J. Clean. Prod.* **2019**, *239*, 117946.

(3) Fan, J.; Sun, Y.; Li, X.; Zhao, C.; Tian, D.; Shao, L.; Wang, J. Pollution of organic compounds and heavy metals in a coal gangue dump of the Gequan Coal Mine, China. *Chin. J. Geochem.* **2013**, *32*, 241−247.

(4) Wu, Y.; Yu, X.; Hu, S.; Shao, H.; Liao, Q.; Fan, Y. Experimental study of the effects of stacking modes on the spontaneous combustion of coal gangue. *Process Saf. Environ. Prot.* **2019**, *123*, 39−47.

(5) Zhang, Y.; Nakano, J.; Liu, L.; Wang, X.; Zhang, Z. Co-combustion and emission characteristics of coal gangue and low-quality coal. *J. Therm. Anal. Calorim.* **2015**, *120* (3), 1883−1892.

(6) Liu, M.; Wen, H.; Fan, S.; Cheng, X.; Liu, W.; Jin, Y. Development of test equipment based on isothermal difference to

https://doi.org/10.1021/acsomega.3c09743
ACS Omega 2024, 9, 14174−14186

determine characteristic parameters involved in coal spontaneous combustion. *Energy Sources, Part A* **2022**, *44* (1), 817−833.
(7) Li, Y.; Ren, X.; Zhang, Y.; Zhang, Y.; Shi, X.; Ren, S. Study on the thermal reaction characteristics and kinetics of coal and coal gangue coexisting spontaneous combustion. *Energy* **2024**, *288*, 129781.
(8) Wu, M.; Li, H.; Wang, L.; Feng, S.; Wang, Y.; Yang, N.; Wang, K.; Yu, M. Investigation on coal/coal gangue mixtures co-combustion via TG-DSC tests, multicomponent reaction model, and artificial neural network. *Fuel* **2024**, *359*, 130443.
(9) Yan, J.; Wu, Y.; Zhang, L.; et al. Synergistic retention of heavy metals and in-situ reduction of NO and SO_2 by co-combustion of sewage sludge and coal gangue: a promising approach for contaminant management and emission reduction. *Fuel Process. Technol.* **2023**, *252*, 107984.
(10) Peng, H.; Wang, B.; Li, W.; Yang, F.; Cheng, F. Combustion characteristics and NO emissions during co-combustion of coal gangue and coal slime in O_2/CO_2 atmospheres. *J. Therm. Sci.* **2022**, *32* (1), 457−467.
(11) Ren, J.; Xie, C.; Guo, X.; Qin, Z.; Lin, J.; Li, Z. Combustion characteristics of coal gangue under an atmosphere of coal mine methane. *Energy Fuel.* **2014**, *28* (6), 3688−3695.
(12) Wang, W.; Wang, P.; Cao, Z.; Cao, Y.; Ma, Y. Experimental study and molecular simulation of spontaneous combustion of coal gangue by oxidation under different water contents. *J. Coal Prep. Util.* **2023**, *43* (12), 2046−2064.
(13) Ran, J.; Niu, B.; Zhang, L.; Pu, G.; Tang, Q. Thermogravimetric study on pyrolysis performance and mechanism of coal residue. *J. China Coal Soc.* **2006**, *31* (5), 640−644.
(14) Pu, F.; Zhang, L.; Wang, J.; Ran, J.; Tang, Q.; Yan, Y. Experimental study on the characteristics of mixed combustion of biomass and coal gangue. *J. Eng. Phys. Thermophys.* **2009**, *30* (2), 333−335.
(15) Wang, M.; Ma, X.; Zhang, Y. Influence of test factors on pyrolysis characteristics of coal gangue. *Fly Ash Compr. Util.* **2011**, No. 2, 37−l43.
(16) Jia, H.; Yu, M. Analysis on the zero-g period and characteristic temperature of coal gangue during adiabatic oxidation process. *J. China Coal Soc.* **2011**, *36* (04), 648−653.
(17) Wang, C.; Wang, D.; Xin, H.; Qi, Z.; Zhang, W.; Zhang, K. Study on secondary oxidation characteristics of coal gangue at different pyrolysis rank. *Fuel* **2023**, *345*, 128231.
(18) Zhang, Y.; Li, W.; Cheng, X.; Yan, K.; Zhao, W.; Yang, F. Air and oxy-fuel combustion characteristics of coal gangue and weathered coal blends. *Energy* **2023**, *284*, 128660.
(19) Zhang, H.; Shu, Y.; Yue, S.; et al. Preheating pyrolysis-char combustion characteristics and kinetic analysis of ultra-low calorific value coal gangue: Thermogravimetric study. *Appl. Therm. Eng.* **2023**, *229*, 120583.
(20) Zhang, Y.; Qi, X.; Zou, J.; et al. Effects of water immersion on the pore structure and thermodynamic properties of coal gangue. *Fuel* **2023**, *346*, 128273.
(21) Jiang, X.; Yang, S.; Zhou, B.; Cai, J. Study on spontaneous combustion characteristics of waste coal gangue hill. *Combust. Sci. Technol.* **2023**, *195* (4), 713−727.
(22) Liu, Y.; Wen, H.; Guo, G.; Jin, Y.; Fan, S.; Cai, G.; Liu, R. Correlation between oxygen concentration and reaction rate of low-temperature coal oxidation: a case study of long-flame coal. *Energy* **2023**, *275*, 127483.
(23) Pi, Z.; Li, R.; Guo, W.; Liu, X.; Zhang, Z.; Wang, Y.; Zhang, Y.; Yin, G.; Li, X. Experimental study on the influence of pore structure and group evolution on spontaneous combustion characteristics of coal samples of different sizes during immersion. *ACS Omega* **2023**, *8* (25), 22453−22465.
(24) Li, B.; Liu, G.; Sun, W.; Ye, L.; Bi, M.; Gao, W. Experimental and theoretical study on kinetic behaviour of coal gangue and raw coal using model reconstruction. *J. Therm. Anal. Calorim.* **2020**, *144* (2), 463−477.
(25) Li, B.; Liu, G.; Gao, W.; Cong, H. Y.; Bi, M. S.; Ma, L.; et al. Study of combustion behaviour and kinetics modelling of Chinese Gongwusu coal gangue: model-fitting and model-free approaches. *Fuel* **2020**, *268*, 117284.
(26) Li, S. The characteristics and kinetic mechanismsof coal residue pyrolysis in the different atmosphere. *Chongqing Univ.* **2009**, 31−32.
(27) Gao, J.; Chang, M.; Shen, J. Comparison of bituminous coal apparent activation energy in different heating rates and oxygen concentrations based on thermogravimetric analysis. *J. Therm. Anal. Calorim.* **2017**, *130*, 1181−1189.
(28) Zhu, H.; Guo, A.; Qu, L. Experimental study on the relationship between thermal kinetic parameters, characteristic temperature and volatilization of coal. *Chin. J. Saf. Sci.* **2012**, *22* (3), 55−60.
(29) Jia, H.; Yu, M. Analysis of the weightlessness phase and characteristic temperature point of coal gangue adiabatic oxidation. *J. Coal Min.* **2011**, *36* (4), 648−653.
(30) Shi, Y.; Yun, F.; Yang, P.; Jia, X.; Song, C. Analysis of the weightlessness phase and characteristic temperature point of coal gangue adiabatic oxidation. *J. Coal Min.* **2011**, *36* (4), 648−653.
(31) Ran, J.; Niu, B.; Zang, L.; Pu, G.; Tang, Q. Study on general combustion performance and kinetic characteristics of combustion of coal residue. *Proc. CSEE* **2006**, *26* (15), 58−62.
(32) Li, Y.; Qiao, Y.; Wang, W.; Wang, Z.; Di, L.; Liu, W. Experimental study on kinetic parameters of coal oxidation under different oxygen concentrations. *Coal Mine Saf.* **2015**, *46* (7), 44−47.
(33) Shi, X.; Wang, Q.; Ma, W.; Wu, D. Effect of reaction atmosphere on pyrolysis performance of flat coal coals. *Coal Convers.* **2014**, *37* (3), 5−9.
(34) Xu, M.; Gao, P.; Men, Z.; Wang, X.; Li, C. Effect of water on the distribution of pyrolytic products in Shendong coal. *Clean Coal Technol.* **2017**, *23* (1), 52−56.
(35) Chang, N.; Gan, Y.; Chen, Y. Effect of heating rate and pyrolysis temperature on coal pyrolysis process. *Coal Convers.* **2012**, *35* (3), 1−5.
(36) Zhou, P.; Wang, N.; Zhou, J.; Xiao, C. Study on characteristic temperature of coal spontaneous combustion process with different grain size by thermogravimetric analysis. *Clean Coal Technol.* **2010**, *16* (3), 64−66.
(37) Xu, B.; Liu, Q.; Ai, B.; Ding, S.; Frost, R. Thermal decomposition of selected coal gangue. *J. Therm. Anal. Calorim.* **2018**, *131*, 1413−1422.
(38) Wang, Y.; Zhang, Y.; Zhou, Q.; Zhang, Y.; Sun, J. Thermal kinetics analysis of coal-gangue selected from Inner Mongolia in China. *J. Therm. Anal. Calorim.* **2018**, *131* (2), 1835−1843.
(39) Bai, Z. *Thermal Analysis Kinetics*; Science Press: Beijing, 2008.
(40) Bai, Y. Study on secondary oxidation characteristics of coal with different preoxidation degree. *J. Xi'an Univ. Eng. Sci. Technol.* **2018**, 81−84.
(41) Zhang, X.; Bai, Y.; Li, Y.; Ma, T. Kinetics and segmentation law of coal oxidation at elevated temperature. *J. Xi'an Univ. Eng. Sci. Technol.* **2017**, *37* (4), 474−478.
(42) Yang, F.; Liu, X. Comparative study on activation energy calculation for coal spontaneous combustion with different thermal gravimetric analysis methods. *Min. Saf. Environ. Prot.* **2016**, *43* (5), 9−13.
(43) Campbell, J. S.; Grace, J. R.; Lim, C. J.; Mochulski, D. W. A new diagnostic when determining the activation energy by the advanced isoconversional method. *Thermochim. Acta* **2016**, *636*, 85−93.
(44) Vyazovkin, S.; Burnham, A. K.; Criado, J. M.; Pérez-Maqueda, L. A.; Popescu, C.; Sbirrazzuoli, N. ICTAC Kinetics Committee recommendations for performing kinetic computations on thermal analysis data. *Thermochim. Acta* **2011**, *520* (1−2), 1−19.
(45) Du, Y. Simulation study on thermodynamic characteristics of spontaneous combustion of high-sulfur gangue mountain. *J. China Univ. Min. Technol.* **2020**, 1−3.
(46) Zhang, Y.; Li, Y.; Huang, Y.; Li, S.; Wang, W. Characteristics of mass, heat and gaseous products during coal spontaneous combustion

https://doi.org/10.1021/acsomega.3c09743
ACS Omega 2024, 9, 14174−14186

using TG/DSC−FTIR technology. *J. Therm. Anal. Calorim.* **2018**, *131* (3), 2963−2974.
(47) Tang, Y.; Wang, H. Laboratorial investigation and simulation test for spontaneous combustion characteristics of the coal waste under lean-oxygen atmosphere. *Combust. Sci. Technol.* **2020**, *192* (1), 46−61.

https://doi.org/10.1021/acsomega.3c09743
ACS Omega 2024, 9, 14174−14186